



Simulation of water-clay flow in dam break with SPH method

H. Lashkarbolouk¹, M.R. Chamani², A.M. Halabiyani², A.R. Pishahvar³

1- MSc of Civil Engineering, Lecturer, Payam-e-Noor University, Gorgan, Iran

2- Department of Civil Engineering, Isfahan University of Technology, Isfahan, Iran

3- Department of Mechanical Engineering, Isfahan University of Technology, Isfahan, Iran

h.lashkarbolok@cv.iut.ac.ir

Abstract

In the field of Civil Engineering, non-Newtonian fluids such as water-cement mix, SCC (Self Compacted Concrete) and bentonite are widely used. In this article, water-clay mix flow in dam break problem is studied numerically. Water-clay mix rheology is assumed as Bingham fluid. As the water-clay mix flow in the dam break problem is a free surface flow with large deformation, SPH method is used for the simulation. To verify the simulation results, the predicted results such as free surface shape and leading edge position have been compared with experimental data. The simulation is then used to determine parameters of motion which are difficult to measure in the laboratory. These results include exciting mass from gate position at each time step, height of fluid at a particular point, and leading edge velocity. The results also indicate that SPH method is accurate enough for simulation of non-Newtonian fluid flow with free surface problems.

Keywords: SPH method, Dam break, Non-Newtonian fluid, Water-clay mix, Bingham fluid.

1. Introduction

Non-Newtonian fluids are widely applied in industry and Civil Engineering. Water-clay mixture, bentonite, and concrete are non-Newtonian fluids which are used in constructing of the structures. To enhance the efficiency in using these materials and their effects on the structures, the reaction between these materials with the structures should be determined. Momentum equations govern for all fluid behavior and flow characteristics such as velocity, pressure, fluid height, and density changes can be predicted. Momentum equations are partial differential equations for which, so far, no exact solution has been found and usually are solved numerically.

The numerical methods are classified into two general groups based on the type of discretizing solution domain. The first group is the mesh-based numerical methods in which the points have a fixed place during the solution such as finite difference method (FDM), finite element method (FEM), and finite volume method (FVM). The other group of numerical methods is known as mesh-less methods. In these methods, the continuum domain of simulation is discretized into finite number of points and can freely move all over the solution domain. These points can have mass, volume, density, and speed. The mesh-less method such as SPH can satisfactorily model the free surface flow problems with large deformation, moving boundary, and problems with complex geometry where the generated mesh is complicated.

In the previous studies, water flow in dam break problem was simulated with SPH method. Leading edge position, water surface shape, and variation of water height at specific locations were determined [1, 2, 3]. Hosseini et al. (2007) presented a new fully explicit SPH algorithm for simulation of power-law, Bingham-plastic, and Herschel-Bulkley fluid flows. The performance of the proposed algorithm is assessed by solving three test cases including a non-Newtonian dam-break problem, flow in an annular viscometer, and a mud fluid flow on a sloping bed. The results obtained were in close agreement with the available experimental and numerical data [5]. Lee et al. (2010) applied two algorithms of the SPH method (weakly compressible and truly incompressible algorithm) for simulation of two problems; i.e., water column collapsing in a rectangular tank, and ski-jump spillway downstream of a dam reservoir. They concluded that the incompressible algorithm model predicts flow characteristics more accurately compared to weakly compressible algorithm predictions [4].

In the present investigation, the dam break of the water-clay mixture is studied numerically. The gate



is removed instantaneously and the water-clay mixture begins to move. The Navier-Stokes equation for non-Newtonian fluid in the Lagrangian viewpoint is discretized using the mesh-less SPH method.

2. Numerical Modeling

2.1. Governing equations

Lagrangian governing equations for a two dimensional incompressible flow are expressed as

$$\frac{D\rho}{Dt} + \rho \nabla \cdot v = 0 \quad \text{Continuity equation} \quad (1)$$

$$\frac{Dv^\alpha}{Dt} = \frac{1}{\rho} \frac{\partial}{\partial x^\beta} (-p \delta^{\alpha\beta} + \tau^{\alpha\beta}) + g \quad \text{Momentum equation} \quad (2)$$

where D/Dt is the material derivative, ρ is the density of fluid, v is flow velocity, g is the acceleration of gravity, α and β denote the coordinate directions (x or y), p is pressure stress, τ is shear stress, and $\delta^{\alpha\beta}$ is the Dirac Delta function [6]. Equations (1) and (2) are applicable for Newtonian and non-Newtonian fluids [7]. It is known that the relations between shear stress and the rate of shear strain for SCC is similar to the Bingham fluid given as

$$\begin{cases} \varepsilon = 0 & |\tau| \leq \tau_B \\ \tau = \left(\frac{\tau_B}{|\varepsilon|} + \mu \right) \cdot \varepsilon & |\tau| > \tau_B \end{cases} \quad (3)$$

where

$$|\tau| = \sqrt{\frac{I}{2} \tau \cdot \tau} \quad \text{and} \quad |\varepsilon| = \sqrt{\frac{I}{2} \varepsilon \cdot \varepsilon} \quad (4)$$

where μ is dynamic viscosity, τ_B is the yield stress of fluid, ε is the rate of shear strain, $|\tau|$ and $|\varepsilon|$ are the second invariants of the extra stress and strain rate, respectively. The fluid acts like a rigid matter for shear stress less than a critical value of τ_B [8].

2.1.1. Equation of state

In the SPH method, the pressure (p) is expressed by the equation of state as $p = p(\rho, c)$, where ρ is particle density and c is the speed of sound. The state equation employed in this study is the Tait's state equation and is expressed as

$$p = \frac{c^2 \rho}{\gamma} \left[\left(\frac{\rho}{\rho_0} \right)^\gamma - 1 \right] \quad (4)$$

where ρ_0 is the reference density and the value of $\gamma = 7$. Generally, the oscillation of density in incompressible fluid in numerical methods is allowed up to 1%. In SPH method, it is recommended that the speed of sound be considered 10 times more than the maximum speed of the fluid for an incompressible flow [9, 10].

2.2 SPH formulation

SPH method divides the domain of solution into a number of discrete particles (N). These particles have a spatial distance (h) over which their properties are smoothed by a kernel function. Method of interpolation in SPH is an integral descriptive method and the spatial variable is approximated using the available information in the local area around the desired point. In SPH method, discretization form of variable f and its derivative will be as follows

$$\langle f(x_i) \rangle = \sum_{j=1}^N \frac{m_j}{\rho_j} f(x_j) W_{ij} \quad ; \quad [W_{ij} = W(x_{ij}, h)] \quad (5)$$



$$\langle \nabla \cdot f(x_i) \rangle = \sum_{j=1}^N \frac{m_j}{\rho_j} f(x_j) \nabla_i W_{ij} \quad ; \quad \left[\nabla \cdot W_{ij} = \frac{dW}{dr_{ij}} \frac{1}{|r_{ij}|} [(x_i - x_j) \hat{i} + (y_i - y_j) \hat{j}] \right] \quad (6)$$

where f is a function of the three-dimensional position vector x , i is for the desired particle which the unknown variable is calculated, j are for particles which are placed inside the influence domain of particle i , h is the smoothing length which defines the influence domain of kernel function, m_j is the mass of the particle, and $W(x_{ij}, h)$ is the kernel function [11]. The value of $f(x_i)$ for the i^{th} point is approximated within the particles in the influence domain of the i^{th} particle. The kernel function is normalized over its influence domain where outside this domain, the kernel function gets zero value and within that domain, it gets a positive value. In this study, a 3rd order and two dimensional kernel function is used as

$$W(R) = \alpha_d \times \begin{cases} \frac{2}{3} - R^2 + \frac{1}{2} R^3 & \text{if } 0 \leq R < 1 \\ \frac{1}{6} (2 - R)^3 & \text{if } 1 \leq R < 2 \\ 0 & \text{if } R \geq 2 \end{cases} \quad ; \quad [R = |x_i - x_j|/h] \quad (7)$$

The values of α_d for one, two and three dimensional simulations are $1/h$, $15/7\pi h^2$, and $3/2\pi h^3$, respectively [12].

2.2.1. Discretization

The derivation of the basic SPH form of Eq. (1) is given as

$$\frac{D\rho_i}{Dt} = \sum_{j=1}^N m_j v_{ij}^\beta \frac{\partial W_{ij}}{\partial x_i^\beta} \quad (8)$$

where v_{ij} is the difference of the velocities of particles i and j in all directions, and $\partial W_{ij}/\partial x_i^\beta$ is the derivation of the kernel function in the considered direction [7]. Eq. (2) is discretized as

$$\frac{Dv_i^\alpha}{Dt} = - \sum_{j=1}^N m_j \frac{p_i + p_j}{\rho_i \rho_j} \frac{\partial W_{ij}}{\partial x_i^\beta} + \sum_{j=1}^N m_j \frac{\mu_i \varepsilon_i^{\alpha\beta} + \mu_j \varepsilon_j^{\alpha\beta}}{\rho_i \rho_j} \frac{\partial W_{ij}}{\partial x_i^\beta} + \Pi_{ij} \quad (9)$$

where Π_{ij} is the artificial viscosity. The right hand side terms of Eq. (9) are the SPH approximation of pressure and the existence of viscous forces, respectively, the term $\varepsilon_i^{\alpha\beta}$ is written, based on its discrete definition, as

$$\varepsilon_i^{\alpha\beta} = \sum_{j=1}^N \frac{m_j}{\rho_j} v_{ji}^\beta \frac{\partial W_{ij}}{\partial x_i^\alpha} + \sum_{j=1}^N \frac{m_j}{\rho_j} v_{ji}^\alpha \frac{\partial W_{ij}}{\partial x_i^\beta} - \left(\frac{2}{3} \sum_{j=1}^N \frac{m_j}{\rho_j} v_{ji} \cdot \nabla_i W_{ji} \right) \delta^{\alpha\beta} \quad (10)$$

Using the Eq. (10) and by calculating strain rate and substituting it in the Eq. (9), the acceleration value of each particle is obtained and thus the speed and location of particle in each time step is found [7].

2.2.2. Artificial viscosity

For preventing the unphysical oscillations in the numerical results and to simulate shock waves, the artificial viscosity in SPH method is used. Many forms of artificial viscosity have been proposed. The Monaghan's type definition for artificial viscosity is as follows

$$\Pi_{ij} = \begin{cases} \frac{-\alpha_\Pi \bar{c}_{ij} \varphi_{ij} + \beta_\Pi \varphi_{ij}^2}{\bar{\rho}_{ij}} & v_{ij} \cdot x_{ij} < 0 \\ 0 & v_{ij} \cdot x_{ij} > 0 \end{cases} \quad (11)$$

where

$$\varphi_{ij} = \frac{h \cdot v_{ij} \cdot x_{ij}}{|x_{ij}|^2 + 0.01h^2} \quad ; \quad \bar{c}_{ij} = \frac{c_i + c_j}{2} \quad ; \quad \bar{\rho}_{ij} = \frac{\rho_i + \rho_j}{2} \quad ; \quad v_{ij} = v_i - v_j \quad ; \quad x_{ij} = x_i - x_j \quad (12)$$

The first term in Eq. (11) associated with α_Π produces a bulk viscosity, while the second term associated with β_Π is for keeping the particle interpenetration. The values of α_Π and β_Π in Eq. (12), are set approximately



equal to 1. The $0.01h^2$ term is inserted to prevent numerical divergence when two particles are approaching each other [13].

3. Simulation of non-Newtonian fluid flow in dam break problem

The water-clay mix was considered in the simulation of the non-Newtonian dam break problem which the relation between shear stress and strain rate is governed by the Bingham fluid. The experimental model specification are set as $L = 2$ m, $H = 0.1$ m, and $S = 0.1\%$ where L and H are, respectively, length and height of water-clay mixture upstream the gate, and S is bed slope (Fig. 1). The rheological properties for this mixture is $\tau_0 = 25$ Pa, $\mu = 0.07$ Pa.s, and $\rho = 1200$ kg/m³ [1].

For the verification of the results using the SPH method, it is necessary to determine appropriate number of particles. The simulation begins with few particles and the number is increased in the succeeding simulations until the simulation results don't change considerably for more particles. This procedure can be done with reduced dimensions of the model to save time. The length of model is reduced to $L = 1$ m. In this state, the simulations were done with 250, 1000, 2250, 4000 particles which are equal to 500, 2000, 4500, and 8000 particles in the main model. Figure 2 shows the simulation results for leading edge position for various numbers of the particles. It is shown that output results for leading edge position in simulation with 2250 particles is close to results of 4000 particles. For more particles, the results of the simulation will not considerably change. The results for the position of leading edge with the 1000 particles are around the results of the simulation with 2250 and 4000 particles. The computers with four cores processor and 3.25 GB RAM need to 12 hours for the simulation of 1 second of the model with 2250 particles. As such computer requires 10 days to simulate 10 seconds of the fluid flow in the main model with 4500 particle. Consequently, 2000 particles are chosen for simulation of the main model (simulation of main model with 2000 particles is equal to simulation with 1000 particles for the reduced model). The solution geometry is divided into 10×200 particles where the distance of the particles from each other is 10 mm. The left side boundary which is 0.2 m is discretized into 40 particles and the bottom boundary which is chosen as 4 m with $S = 0.1\%$ is discretized into 800 particles with a distance of 5 mm from each other. The gate is lifted instantaneously and the fluid begins to move. The simulation continues till the fluid stops moving. Figure 3 indicates the results of simulation for times of 0.3, 0.6, 1, and 3 seconds after the removal of the gate. The results obtained by the numerical solution of the leading edge position and the laboratorial data are compared and indicated in Fig. 4. The comparison shows that the output results of simulation agree well with the laboratorial data [1].

To determine the stoppage time of the non-Newtonian flow simulation, the function of root mean square (RMS) is used. For value of $RMS = -3$, the average velocity changes in the particles is about 0.001 m/s which is negligible. In Fig. 5, the variation of RMS function for flow velocity is shown. This figure shows that at $t = 6$ sec, the RMS function has reached the value of -3 which indicates that the motion of the fluid can be assumed as the stoppage time. The fluid free surface profile is also shown in Fig. 6 for different time after lifting the gate is well predicted by SPH method.

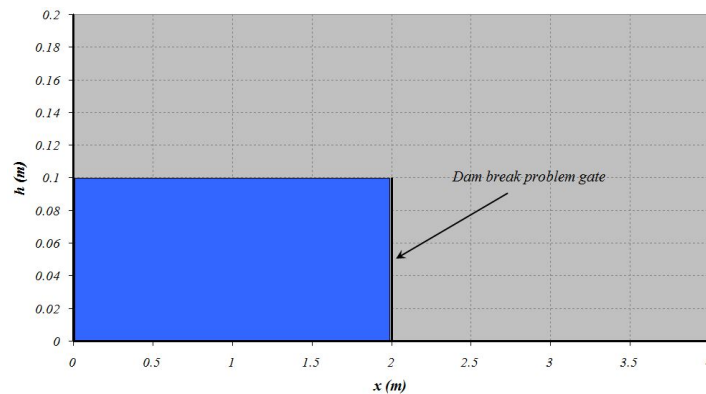


Figure 1. Geometry of dam break problem.

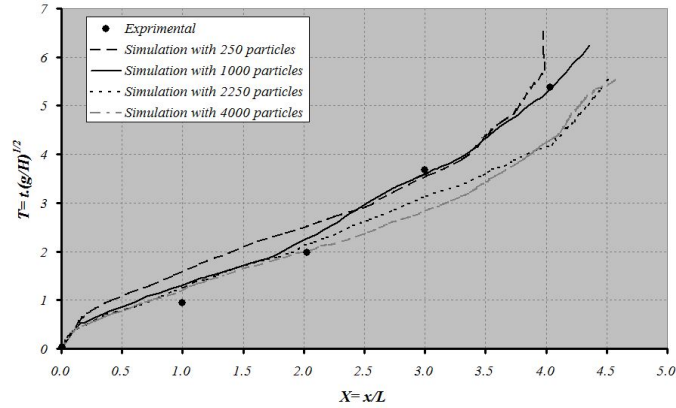


Figure 2. Leading edge position in simulation with different number of particle.

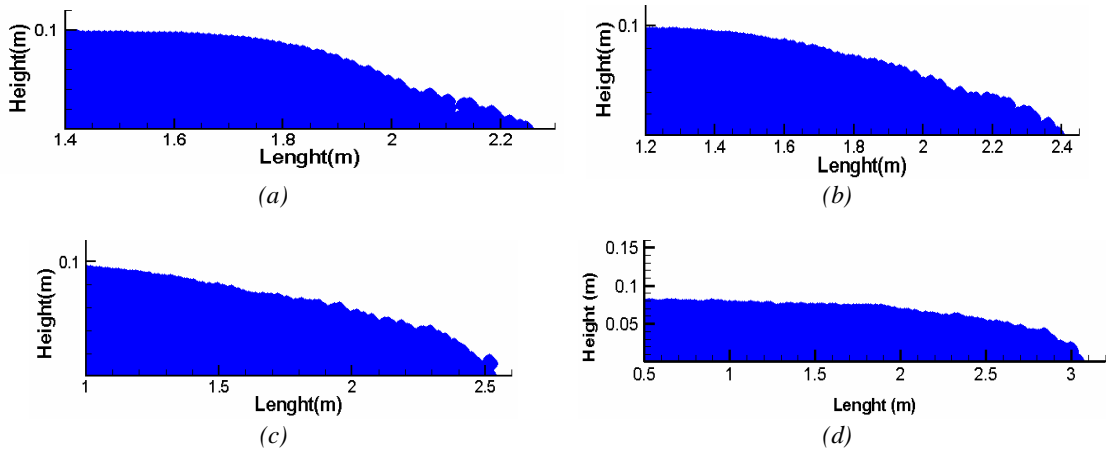


Figure 3. Water-clay mix flow in dam break problem at different times; a) 0.3 sec, b) 0.6 sec, c) 1 sec, d) 3 sec.

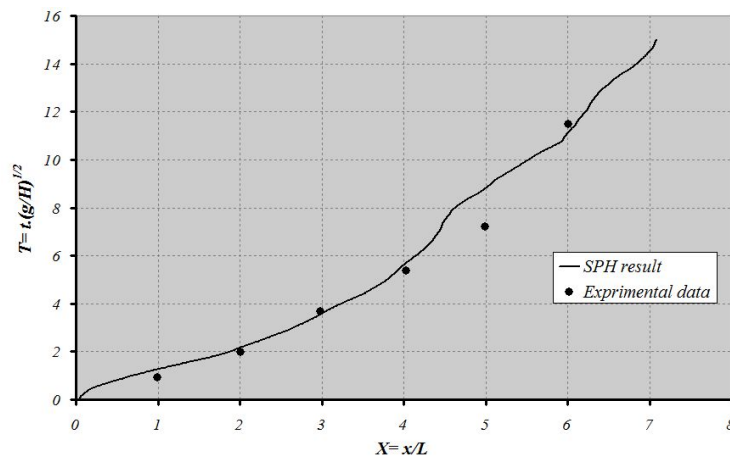


Figure 4. Leading edge position.

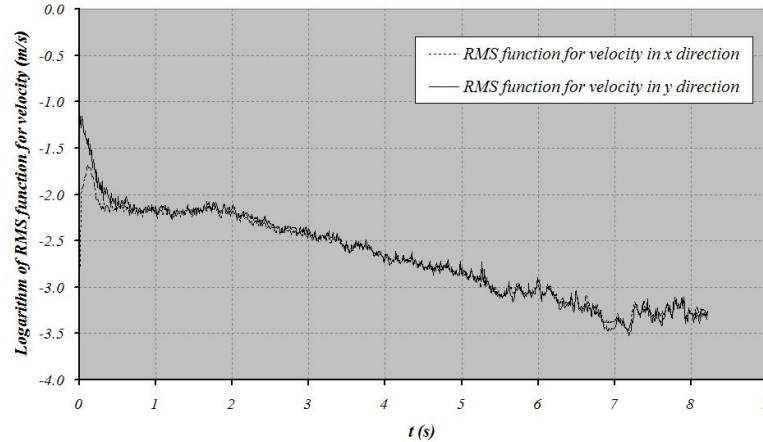


Figure 5. RMS function for velocity in x and y direction.

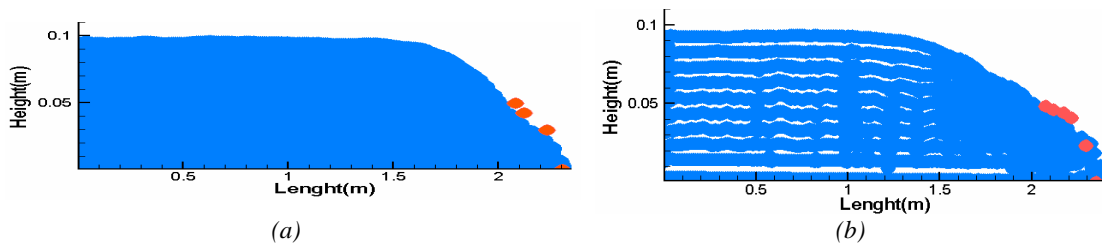


Figure 6. Water-clay mix free surface profile at different times after the removal of the gate; a) 0.37 sec, b) 0.67 sec (Blue points are SPH particles and red point are experimental data).

Considering the analysis carried out so far, we can conclude that SPH method has a good precision in solving the governing equations and simulation of the non-Newtonian fluid flow. More flow characteristics can be obtained by this method which are difficult and costly to be produced in experimental works. In Fig. 7, the variation of the leading edge velocity has been indicated. It is concluded that leading edge velocity increases up to $t = 0.17$ sec and decreases after this time.

In Figs. 8 and 9, the changes of the mass and height of the fluid have been shown in upstream the gate. Figure 8 indicates that the mass of fluid is reduced up to $t = 0.4$ sec whereafter it gets a constant value. This subject complies with the facts that the mass decreases in the upper section of gate due to decrease of fluid height and after $t = 0.4$ sec, the fluid height is fixed and the mass changes become stable. The same conclusion is held for the height change of fluid at the gate section (Fig. 9). Also we can use Lagrangian property of SPH method for tracking down the path line of a special particle during the simulation process. Concerning the fluid flow and model the route of the special particle motion, velocity, and pressure change. In Fig. 10, a particle path line with initial position at $L = 1.99$ m and $H = 0.03$ m has been indicated during three seconds after opening of the gate.

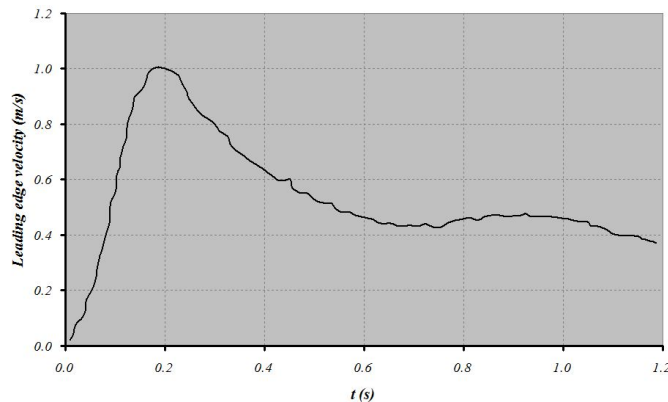


Figure 7. Leading edge velocity.

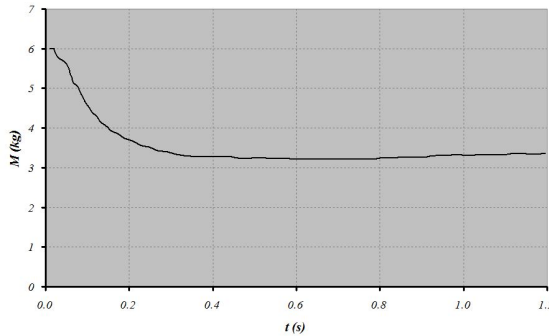


Figure 8. Change of fluid mass at the gate section.

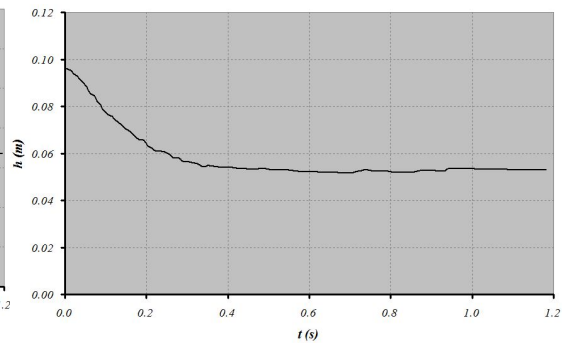


Figure 9. Change of fluid height at the gate section.

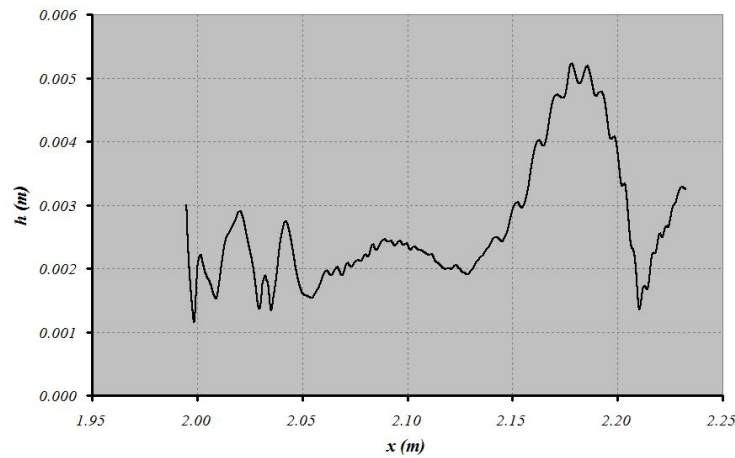


Figure 10. Path line for a particle at initial position with $L = 1.99$ m and $h = 0.03$ m for 2.25 seconds after the gate removal.

4. Conclusion

In this study, the water-clay mix flow was simulated in dam break problem using SPH method. Water-clay mix was assumed a non-Newtonian fluid of Bingham model. After determining the appropriate number of particles for solving the equations and simulation of fluid flow, the output results such as leading edge position and the profile of the fluid surface were compared with experimental data. It is concluded that SPH method is able to well simulate the flow of non-Newtonian fluids with free surface flow problems. More characteristics of water-clay mix flow in the dam break problem such as shape of fluid surface, change of fluid mass, and height of fluid at a specific section are obtained which are difficult and costly to obtain in the laboratory.

5. Reference

1. Shao, S. and Lo, E. Y. M. (2003), "Incompressible SPH method for simulating Newtonian and non-Newtonian flows with a free surface," *Advances in Water Resources*, 26, pp. 787-800.
2. Groenenboom, P. H. L. and Cartwright, B. K. (2010), "Hydrodynamics and fluid-structure interaction by coupled SPH-FE method," *Journal of Hydraulic Research*, 48 (EI), pp. 61-73.
3. Hughes, J. P., David, I. and Graham, D. I. (2010), "Comparison of incompressible and weakly-compressible SPH models for free-surface water flows," *Journal of Hydraulic Research*, 48 (EI), pp. 105-117.



4. Lee, E. S., Violeau, D., Issa, R. and Ploix, S. (2010), "Application of weakly compressible and truly incompressible SPH to 3D water collapse in waterworks," *Journal of Hydraulic Research*, 48 (E1), pp. 50–60.
5. Hosseini, S. M., Manzari, M. T. and Hannani, S. K. (2007), "A fully explicit three-step SPH algorithm for simulation of non-Newtonian fluid flow," *Journal of Numerical Methods for Heat and Fluid Flow*, 17 (7), pp. 715-735.
6. Ancey, C. and Cochard, S. (2009), "The dam-break problem for Herschel–Bulkley viscoplastic fluids down steep flumes," *Journal of Non-Newtonian Fluid Mechanics*, 158 (1-3), pp. 18-35.
7. Liu, J. R. and Liu, M. B. (2003), "Smoothed Particle Hydrodynamics: a meshfree particle method," World Scientific Publishing Co, Singapore.
8. Smyrniotis, D. N. and Tsamopoulos, J. A. (2001), "Squeeze flow of Bingham plastics," *Journal of Non-Newtonian Fluid Mechanics*, 100 (1-3), pp. 165–190.
9. Lopez, D., Marivela, R. and Garrote, L. (2010), "Smoothed particle hydrodynamics model applied to hydraulic structures: a hydraulic jump test case," *Journal of Hydraulic Research*, 48 (E1), pp. 142–158.
10. Gomez-Gesteria, M., Rogers, B. D., Dalrymple, R. A. and Crespo, A. J. C. (2010), "State-of-the-art of classical SPH for free-surface flows," *Journal of Hydraulic Research*, 48 (E1), pp. 6–27.
11. Bui, H. H., Sako, K. and Fukagawa, R. (2007), "Numerical simulation of soil–water interaction using smoothed particle hydrodynamics (SPH) method," *Journal of Terramechanics*, 44 (5), pp. 339–346.
12. Fang, J., Parriaux, A., Rentschler, M. and Ancey, C. (2009), "Improved SPH methods for simulating free surface flows of viscous fluids," *Applied Numerical Mathematics*, 59 (2), pp. 251–271.
13. Mehra, V. and Chaturvedi, S. (2006), "High velocity impact of metal sphere on thin metallic plates: A comparative smooth particle hydrodynamics study," *Journal of Computational Physics*, 212 (1), pp. 318–337.